Comprehensive distributed parameter model of an upflow anaerobic sludge bed (UASB) reactor

S.J. Mu [a], Y. Zeng[a], B. Tartakovsky [b], S.J. Lou [b], S. R. Guiot [b], P. Wu[a]*

a Institute of High Performance Computing, 1 Science Park Road, #01-01, The Capricorn, Singapore 117528
b Biotechnology Research Institute, NRC, 6100 Royalmount Ave, Montréal, Québec, Canada H4P 2R2
[*] *Corresponding author*

Abstract

In the present work, IWA Anaerobic Digestion Model No. 1 (ADM1) is used as a basis for developing a comprehensive distributed parameter model of the UASB reactor. Material balances of ADM1 are transformed to a set of partial differential equations (PDEs) describing hydraulics and biotransformation phenomena in the UASB reactor. The orthogonal collocation method is applied to solve the distributed PDEs model. Parameter estimation of the model is carried out using a zero-order minimization algorithm of Nelder and Mead yielding a good agreement between model outputs and the measurements. In comparison to CSTR model, the distributed parameter model provides better fitting of the experimental measurements. More importantly, the distributed model allows for studying the influence of upflow velocity on the reactor dynamics and describes spatial distribution of substrates and microorganisms. Conversely, a CSTR model is unable to do so because of the assumption of ideal mixing. Overall, the study suggests that distributed parameter model provides better accuracy in describing the industrial UASB reactors than the CSTR model.

Keywords: UASB reactor; axial dispersion; distributed parameter model; ADM1

Introduction

Upflow anaerobic sludge bed (UASB) reactors are used in anaerobic treatment of high strength wastewaters. Typically, an UASB reactor has a sludge bed thickness of 2-5 m and is operating at a liquid upflow velocity of 1 m h^{-1} or below and a retention time of 8 h or above. Under these operating conditions the existence of significant substrate and biomass gradients in UASB-type reactors might be expected and has been experimentally demonstrated in a number of studies [1-4]. Considerable efforts have been made to study biological and chemical kinetics of the anaerobic digestion process. Recently, a structured model of the anaerobic digestion process, Anaerobic Digestion Model no 1 (ADM1), was proposed by International Water Association (IWA) task group [5]. ADM1 accounts for steps of disintegration, hydrolysis, acidogenesis, acetogenesis, and methanogenesis. It includes 12 substrates, 12 particulars, 9 ions and 3 gas components and 19 biological processes, 6 acid-base equilibrium processes and 3 gas transfer processes [5]. Because of the comprehensiveness of the bioconversion processes in ADM1, the model is applicable for simulating a wide range of anaerobic digestion processes.

Our previous work studied hydraulics of the UASB reactor by using on-line measurements of a fluorescent tracer [4]. In the present work ADM1 model is used as a basis

for developing a comprehensive distributed parameter model of the UASB reactor. Measurements of chemical oxygen demand (COD) and volatile fatty acids (VFAs) are carried out at four reactor heights. In comparison to CSTR model, the distributed model was able to reflect the influence of recirculation flowrate on the reactor dynamics and describe the component gradient along the position, which make it possible to be used in developing new control strategies for UASB reactor, i.e. using recirculation flowrate to reduce the impact of organic overload on UASB reactor removal efficiency.

2. Experiment and methods

Experiments were carried out in a 10.4 L Plexiglas reactor with an internal diameter of 14.3 cm (Figure 1). The reactor was equipped with a water jacket for temperature control, a pH control system, and an external recirculation loop. The reactor was inoculated with granular anaerobic sludge (A. Lassonde Inc., Rougemont, Quebec, Canada) with an average volatile suspended solids content of 50 g L^{-1}. A temperature of 30°C was maintained throughout the experiment. The reactor was fed with a stock solution of synthetic wastewater, which contained (in g L^{-1}): sucrose 99; butyric acid 48; yeast extract 60; ethanol (95%) 35; KH_2PO_4 3; K_2HPO_4 3.5; NH_4HCO_3 34. In each test run, the stock solution was diluted according to the designed organic load to obtain the target wastewater strength. In addition to the synthetic wastewater stream, the influent contained bicarbonate buffer (0.68 g L^{-1} of $NaHCO_3$ and 0.87 g L^{-1} of $KHCO_3$) and microelements. The bicarbonate buffer was used to maintain a hydraulic retention time (HRT) of 10 h. The microelements solution contained (in mg L^{-1}): $AlK(SO_4)$-$12H_2O$ 0.1, H_3BO_3 0.17, $Ca(NO_3)_2$-$4H_2O$ 88.3, $Co(NO_3)_2$-$6H_2O$ 1.2, $Cu(SO_4)$ 0.05, $Fe(SO_4)$-$7H_2O$ 9.0, $MgSO_4$ 32.6, $Mn(SO_4)$-H_2O 2.5, $Na_2(MoO_4)$-$2H_2O$ 0.38, $NiSO_4$-$6H_2O$ 0.12, Na_2SeO_4 0.21, $ZnSO_4$-$7H_2O$ 0.58.

The reactor was equipped with an electronic bubble counter for biogas flow rate measurements. Methane and carbon dioxide contents of biogas were measured on-line using a gas analyzer (Ultramat 22P, Siemens, Germany) interfaced with a personal computer. Reactor pH was stabilized to pH 7 by computer controlled addition of 0.5 N NaOH. Four experiment scenarios were designed by changing the recirculation flowrate and influent OLR at different levels, as shown in Table 1. Each experiment test was performed for 7 days to guarantee the steady state.

Table 1. Experimental conditions

Set #	1	2	3	4
Duration time, (day)	1-7	8-14	15-21	21-28
Upflow velocity (m h^{-1})	0.15	0.83	0.32	0.32
Organic Loading Rate (g L^{-1} d^{-1})	60	60	60	100
Input Flow Rate(L h^{-1})	1.04	1.04	1.02	1.02
External recirculation Rate (L h^{-1})	1.37	12.37	4.12	4.12
Operating Temperature (K)	308.15	308.15	308.15	308.15
Dilution Water Flow Rate, (L d^{-1})	24.08	24.08	23.65	23.64

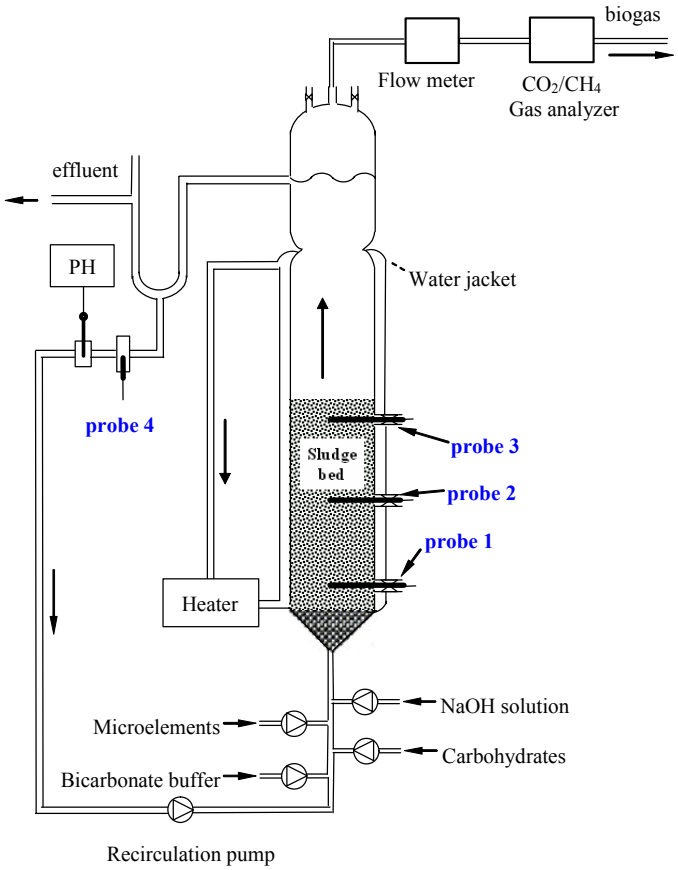

Figure 1. A schematic diagram of the experimental setup. Sampling devices used for fluorescence measurements at different reactor heights are shown as probes 1-4.

Liquid samples were collected from four sampling ports and centrifuged for 10 minutes at 10,000 rpm, to remove solids. The centrifuged samples were then analyzed for COD and VFA content. COD were determined according to Standard Methods [6]. VFAs were measured using a gas chromatograph (Sigma 2000, Perkin-Elmer, Norwalk, USA) equipped with a 91*cm* x 4*mm* i.d. glass column packed with 60/80 Carbopack C/0.3% Carbopack 20 NH_3PO_4 (Supelco, Canada). The column temperature was maintained at 120^{o}C, while the injector and detector temperature was 200 ^{o}C. The carrier gas was nitrogen.

MODELING FRAMEWORK

The distributed parameter model was developed on the basis of Anaerobic Digestion Model No. 1 [5] and thus was called ADM1D. The distributed model considered same components as ADM1, namely soluble organic matter, suspended particulate matter, ions, gas components and biological and chemical kinetics.

Biodegradation kinetics

Kinetic dependencies describing biotransformation of organic matter and growth of microorganisms were adopted from ADM1 [5]. ADM1 assumes that complex solids are

disintegrated into inert substrates, carbohydrates, proteins and fats. Then these products are hydrolyzed to sugars, amino acids and long chain fatty acids (LCFA), respectively. Sugars and amino acids, which are produced from carbohydrates and proteins, are fermented to generate propionate, butyrate, valerate, acetate and hydrogen. LCFA degrade to acetate and hydrogen. Propionate, butyrate and valerate are further degraded to acetate and hydrogen. The final product methane is produced by both the degradation of acetate and the reduction of carbon dioxide by hydrogen.

In addition to the particulate substrates, particulate species also contain active biomass species [7]. The biomass growth kinetics includes growth of microorganisms through the degradation of organic matter and the biomass decay. The rates of biomass growth are proportional to those of the degradation of organic matter, and the biomass decay rates are described by the decay of seven microorganisms. The kinetics also accounts for biomass activity inhibition by some compounds. The inhibition effect is the impairment of a particular bacterial or microorganism function [8]. In ADM1, the inhibition effects of pH, hydrogen, NH3 and LCFA are taken into account.

Material balances

For an axially dispersed tubular reactor the material balance of each component in the liquid phase takes the following form [1, 4]:

$$\frac{\partial c_i}{\partial t} = \frac{\partial}{\partial z}(D_i(z,t).\frac{\partial c_i(z,t)}{\partial z}) - \frac{\partial}{\partial z}(u_i(z,t).c_i(z,t)) + r_i(z,t) \quad (1)$$

where c_i is the soluble matter (S_i, i=1,…,12) or the suspended particulate matter (X_i, i=1,…,12) or ions ($S_{ion,i}$, i=1,…,9). D_i is the dispersion coefficient and u_i is the upflow velocity. The first term characterizes the degree of mixing by fluid flow induced dispersion. The second term determines a convective transport of component c_i in the vertical direction. The third term $r_i(z,t)$ is the net transformation rate for component c_i.

The detailed description of the kinetic dependencies is given in Batstone et al [5].

The Danckwerts boundary conditions [9] for the above liquid component material balance equations are given in the following two equations:

$$D_i(z,t)\frac{\partial c_i}{\partial z} = u_i(z,t)(c_{i(z=0)} - c_{i,in}) \quad z = 0 \quad (2)$$

$$\frac{\partial c_i}{\partial z} = 0 \quad z = H_1 \quad (3)$$

Because biogas bubbles are generated in the process of biodegradation of organic compounds in the liquid phase, biogas transfer occurs on both the interface of gas-liquid phase at the top of the liquid zone and the interface of bubbles and liquid phase along the liquid zone. Therefore, the material balances of biogas compounds are treated as position dependent. The dispersion and convective transport of bubbles in liquid is assumed to be negligible in comparison with the gas transfer rate at the corresponding liquid section. i.e. the following

equation is used to describe the concentration changes of the biogas bubbles produced in the liquid phase.

$$\frac{\partial S_{gas,i}(z,t)}{\partial t} V_{gas} = \frac{\partial}{\partial z}(r_{T,i}(z,t).V_{liq}(z)) - \frac{\partial}{\partial z}(q_{gas}(z,t).S_{gas,i}(z,t)) \quad (4)$$

where *i* denotes material balances for H_2, CH_4 and CO_2. $V_{liq,j}(z)$ is the volume within the reactor height of *dz* where biogas bubble is produced in the liquid phase; $q_{gas,j}$ is the flow rate of biogas bubble produced in $V_{liq,j}(z)$.

$$q_{gas}(z,t) = \frac{RT_{oper}}{P_{atm} - p_{gas,H_2O}} .V_{liq}(z)(\frac{r_{T,H_2}(z,t)}{16} + \frac{r_{T,CH_4}(z,t)}{64} + r_{T,CO_2}(z,t)) \quad (5)$$

The boundary conditions of the gas components are approximated by equalizing the concentrations at the two ends of reactor (i.e. z= 0 and z = 1) to those of their nearest internal points within the reactor.

The schematics of UASB reactor structure with external recirculation flow rate is illustrated in Figure 1. The overall mass balances are given as below.

$$q_{in} + q_{rec} = Q \quad (6)$$

$$q_{in} c_{i,in} + q_{rec} c_{i,r} = Q c_{i,0} \quad (7)$$

where q_{in}, q_{rec} and Q are the flow rates of influent, recirculation and total input flow, respectively. $c_{i,in}$, $c_{i,r}$ and $c_{i,0}$ are the concentrations of i^{th} component in the corresponding stream. Consequently, the model consists of 36 partial differential equations (material balance equations for 12 soluble matters, 12 particulate matters, 9 ions and 3 biogases), 72 ordinary differential equations (two boundary conditions for 36 components) and 33 algebraic equations (overall mass balances for 33 liquid components) which will be solved by a numerical algorithm.

Axial dispersion coefficient

The axial dispersion coefficients [m^2 $h^{-}1$] of all the components were calculated with the relationship reported in our previous study [4].

$$D = D_0 \times u^{1.11} \times 0.01^{\eta_j} \quad (8)$$

where η is the normalized height (liquid phase) defined as $\eta = z / H_1$, D_0 is the dispersion coefficient at η=0, and *u* is the upflow velocity.

For all soluble substrates and ions the same D_0 value was assumed, D_0 = 0.1. For particulates, D_0 was chosen as a smaller value, $D_{0,x}$ = 1.0e-3, because of the fact that the particulates are affected by the gravitational force.

Biomass washout

In this study, a washout fraction $R_{washout}$ was introduced to describe granule transport as the result of bulk movement and gravitational settling. $R_{washout}$ was defined as the ratio of the suspended solids (SS) washed out at each volume segment to the total SS within the segment. The value of $R_{washout}$ was assumed to be dependent on axial position. The biomass distribution was firstly assumed that it decreases from the sludge bottom to the liquid phase which leads to an increase of the upflow velocity of biomass. Thus a washout term $R_{washout}$ was used to describe granule transport as the result of upflow and gravitational forces. $R_{washout}$ took the form of a hyperbolic tangent function (tanh) which describes the transition from the sludge bed to the liquid phase of the reactor, as shown in Eq. (9).

$$R_{washout,i,j} = \frac{x_{i,j}}{x_{total,j}}[\tanh(\beta(x_{total,j} - x_{\max})) + 1]/2 \quad (9)$$

where $x_{total,j} = \sum x_{i,j}$ (total biomass at each position of the reactor). The threshold x_{max} was further defined in Eq. (10) which also took the hyperbolic tangent function, where $Bio_{\max}$ and $Bio_{\min}$ are the maximum and minimum values of the total biomass concentration in the liquid phase respectively, H_j and H_{sludge} are the height at j^{th} position and the sludge height respectively, and β is a constant to be calibrated.

$$x_{\max,j} = 1.45 \times \left[\frac{(Bio_{\max} - Bio_{\min})}{2} \times (1 - \tanh(\beta(H_j - H_{sludge}))) + Bio_{\min} \right] \quad (10)$$

The use of Eqs (9) and (10) well simulate the biomass washout. As shown in Eq. (10), the threshold x_{max} reaches the maximum value at the bottom while at its minimum at the top of the sludge bed. Consequently, the $R_{washout}$ reaches the minimum or approaching to zero at the bottom. In this case, the biomass upflow becomes zero and the sludge bed is held. In contrast, the threshold x_{max} decreases along the reactor height in the liquid phase as calculated by Eq. (10). For given x_{total} that is above the threshold, $R_{washout}$ increases and approaches to $x_{i,j}$ / $x_{total,j}$. This simulates the scenario that the upflow velocity of biomass near the reactor outlet equals to the liquid upflow velocity**,** and biomass would be washed out completely**.**

Numerical methods

The material balance of the axial dispersion model, i.e. Eq. (1), is rewritten with orthogonal collocation representation [10] as following.

$$\frac{dc_{i,j}}{dt} = \frac{1}{HRT_i}\left[\frac{1}{Pe_i} \sum_{k=1}^{N+2} B_{j,k} c_{i,k} - (\frac{dD_i}{d\eta} - \frac{u_i}{H_1}) \sum_{k=1}^{N+2} A_{j,k} c_{i,k} \right] + r_{i,j} \quad (11)$$

where $c_{i,j}$ denotes i^{th} liquid component in the ADM1 system (i = 1,…,33) at j^{th} collocation point (j = 1,…, N), and N is number of the internal collocation points. $A_{(N+2)\times(N+2)}$ and $B_{(N+2)\times(N+2)}$ are the orthogonal collocation matrices for the first and second order derivates, respectively.

Accordingly, the boundary condition equations (Eqs. 2-3) in the collocation method form are represented as below.

$$\frac{1}{Pe_i}\sum_{k=1}^{N+2} A_{1,k}c_{i,k} + c_{i,0} - c_{i,1} = 0 \tag{12}$$

$$\sum_{k=1}^{N+2} A_{N+2,k}c_{i,k} = 0 \tag{13}$$

PARAMETER ESTIMATION AND MODEL VALIDATION

Biological chemical kinetic parameters

Stoichiometric parameters are independent of reactor configurations, and determined by the balance of elements and reaction mechanism. Thus, the distributed model adopted the stoichiometric parameters of ADM1. The details for estimating stoichiometric coefficients can be found in [5]. The hydraulic parameters have been evaluated in our previous study [4]. Thus, only biochemical parameters were estimated in this work. Furthermore, only soluble substrates were measured in the experiment. Hence, the disintegration and hydrolysis constants were not considered for estimation, and were also adopted from the ADM1 benchmark values.

As mentioned above, the soluble COD in ADM1 model includes 7 components, i.e., sucrose, amino acid, long chain fatty acid, valerate, butyrate, propionate and acetate. In ADM1, each substrate degradation process was described by a Monod equation [5], each of which contains two kinetic parameters: the half velocity rate constant $K_{s,i}$ and the maximum specific uptake rate $k_{m,i}$. The VFAs in the model included valerate, butyrate, propionate and acetate, but the valerate and the butyrate shared the same kinetic parameters as $K_{s,c4}$ and $k_{m,c4}$. In this study, only butyrate, propionate and acetate were measured experimentally. Thus, the half velocity rate constants, $K_{s,i}$, and the maximum specific uptake rates, $k_{m,i}$, of the above six substrates (except valerate) were initially considered for estimation for the distributed parameter model (Table 2).

In anaerobic digestion, the degradation/consumption rate of sugar, amino acid, fatty acid, butyrate (or valerate), propionate, acetate and hydrogen were affected by the inhibition effects from NH_3/inorganic nitrogen, pH and H_2. The inhibition effect of NH_3/inorganic nitrogen was related to the parameters of half-saturation constant ($K_{S,IN}$) and the 50% inhibitory concentrations ($K_{I,NH3}$) controlled. The H_2 inhibition was related to the parameters of the 50% inhibitory concentrations of hydrogen on long chain fatty acid ($K_{I,h2,fa}$), butyrate/valerate ($K_{I,h2,c4}$) and propionate ($K_{I,h2,pro}$). In our experiment, pH is maintained to be around 7. Then no pH inhibition effect was considered.

The biogas flowrate was one of the key experimental measurements. It is related to the liquid to gas phase transfer rate, so the gas-liquid transfer constant k_{La} was estimated. Henry's law coefficients of hydrogen ($K_{H,H2}$), methane ($K_{H,CH4}$) and carbon dioxide ($K_{H,CO2}$) also affect gas-liquid transfer rate and flowrate. Among them, the methane component was of particular interest. Hence, four gas-liquid transfer related parameters were considered for estimation.

In summary, there were a total of twenty-one kinetic parameters selected initially for estimation, as listed in Table 2.

Table 2. Estimated kinetic parameter set

No.	Kinetic parameter	Benchmark value	reference value (initial value)	ADM1D value	ADM1 value	units
1	$k_{m,aa}$	50	-	-	-	d^{-1}
2	$K_{S,aa}$	0.3	-	-	-	$kg\ COD\ m^{-3}$
3	$k_{m,fa}$	6	-	-	-	d^{-1}
4	$K_{S,fa}$	0.4	-	-	-	$kg\ COD\ m^{-3}$
5	$k_{m,c4}$	20	**6**	**5.6**	**12**	d^{-1}
6	$K_{S,c4}$	0.2	-	-		$kg\ COD\ m^{-3}$
7	$k_{m,pro}$	13	**1**	**1.7**	**4.5**	d^{-1}
8	$K_{S,pro}$	0.1	-	-	-	$kg\ COD\ m^{-3}$
9	$k_{m,su}$	30	-	-	-	d^{-1}
10	$K_{S,su}$	0.5	-	-	-	$kg\ COD\ m^{-3}$
11	$k_{m,ac}$	8	**1**	**1.5**	**1.8**	d^{-1}
12	$K_{S,ac}$	0.15	-	-	-	$kg\ COD\ m^{-3}$
13	k_{La}	200	**200**	**248**	**250**	$Mliq\ bar^{-1}$
14	$K_{H,h2}$	7.38e-4	-	-	-	$Mliq\ bar^{-1}$
15	$K_{H,ch4}$	0.00116	-	-	-	$Mliq\ bar^{-1}$
16	$K_{H,CO2}$	0.0271	**0.0271**	**0.0232**	**0.0270**	$Mliq\ bar^{-1}$
17	$K_{S,IN}$	0.0001	-	-	-	M
18	$K_{I,nh3}$	0.0018	-	-	-	M
19	$K_{I,h2,fa}$	5e-6	-	-	-	$kg\ COD\ m^{-3}$
20	$K_{I,h2,c4}$	1e-5	-	-	-	$kg\ COD\ m^{-3}$
21	$K_{I,h2,pro}$	3.5e-6	-	-	-	$kg\ COD\ m^{-3}$

Sensitivity analysis of model parameters

The available experimental data were insufficient for estimating twenty one kinetic parameters listed in Table 2. The local relative sensitivity analysis method [11] was employed to select the most sensitive parameters. The sensitivities was quantified in terms of the variation of six process variables under the perturbation of the above twenty one kinetic parameters in their neighbourhood domain. The six process variables were soluble COD, acetate, propionate, butyrate, biogas flowrate and CH_4 percentage. In practice, the calculation employed the finite difference approximation [11] to evaluate sensitivity function as shown in Eq. (14). The perturbation factor δ was set to 1% for all calculations

$$T_{ij} = \frac{\partial C_i / C_i}{\partial p_j / p_j} \approx \frac{(C_i(t, p_j + \delta p_j) - C_i(t, p_j)) / C_i(t, p_j)}{\delta p_j / p_j} \tag{14}$$

where C_i ($i=1,\ldots,4$) denotes the normalized effluent substrate concentration for the i^{th} data set at any process time; p_j is the j^{th} model kinetic parameter, $j=1,\ldots,21$; T_{ij} is the dimensionless sensitivity value of the i^{th} measurement with respect to the j^{th} kinetic parameter.

For the local relative sensitivity analysis, a set of parameter values was determined as the reference values, as listed in fourth column of Table 2. The resultant local sensitivity values of the six process variables to the twenty one parameters are shown in Figure 2.

The sensitivity analysis showed that the maximum specific uptake rate was more significant than the half velocity rate constant for almost all output variables. Figure 2 shows that the maximum specific uptake rates of acetate ($k_{m,ac}$), propionate ($k_{m,pr}$) and butyrate/valerate ($k_{m,c4}$) are inversely proportional to their corresponding half velocity rate constant ($K_{S,ac}$, $K_{S,pr}$ ad $K_{S,c4}$) , respectively on the outputs of soluble COD, acetate, propionate and butyrate. The Henry's law coefficient for CO_2 ($K_{H,CO2}$) and the gas-liquid transfer coefficient (k_{La}) had larger sensitivity values on the biogas flowrate (q_{gas}) and the CH_4 concentration than other parameters. Therefore, $k_{m,ac}$, $k_{m,pr}$, $k_{m,c4}$, k_{La} and $K_{H,CO2}$ were selected from sensitivity analysis to be key parameters for further estimation. Other fifteen parameters were adopted from the benchmark values.

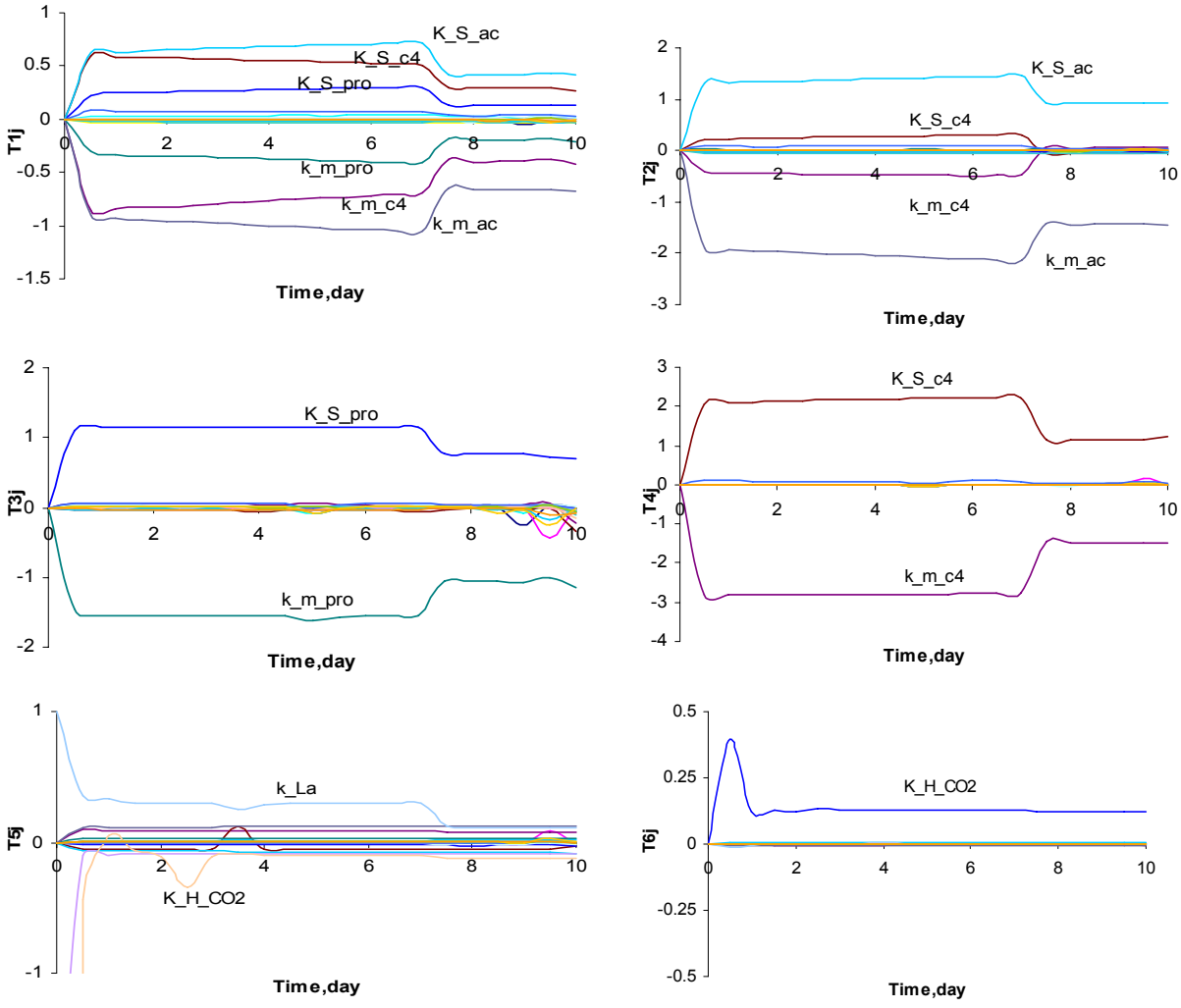

Figure 2 sensitivity analysis of 14 model parameters on 6 model outputs

Parameter estimation objective

The parameters of the distributed model were estimated by minimizing the difference between the experimental measurements (38 samples) and the model calculations of six process variables (soluble COD, butyrate, propionate, acetate, methane percentage and biogas flowrate) at four sampling ports along the reactor height. The objective function for parameter estimation can be mathematically expressed as follows.

$$F_{obj} = \sum_{i=1}^{6} \sum_{j=1}^{4} \sum_{k=1}^{N_{samp}} (C_{i,j,k}^{cal} - C_{i,j,k}^{\exp})^2 \qquad (15)$$

where, $C_{i,j,k}^{cal}$ and $C_{i,j,k}^{\exp}$ are the model calculation and the experimental measurements of the i^{th} process variable, at the j^{th} sampling port along the reactor height, and at the k^{th} sampling time during the experiment; N_{samp} is the number of samples, 38 in this experiment.

The Simplex minimization algorithm of Nelder-Mead was used for the minimization of the objective function. After 300 iterations, the 5 model parameters were estimated as presented in Table 2. The results were compared with the experimental measurements, as presented in Figure 3. Overall, both the simulated dynamic responses and the steady state values were close to the measurements.

RESULTS AND DISCUSSION

Comparison of CSTR and distributed models

In this subsection, the outputs of ADM1 were compared with those of the distributed parameter model and with the experimental data. The kinetic parameters of the CSTR model were estimated in the same way as for the distributed model using the experimental data. The parameter estimation results are given in Table 2. Figure 4 shows measured effluent concentrations and the simulated results using the CSTR model. The CSTR model simulated homogeneous condition inside the reactor, and could not give substrate distribution profile. Also Figure 4 shows that the CSTR model responded to a change in organic loading rate, but not to the changes in the recirculation flowrate.

Substrate and biomass distribution in the reactor

The distributed model was used to analyze the experimental data by examining the axial distribution of substrates and microorganisms. Figure 3 shows simulated and experimentally measured profiles of soluble COD, acetate, propionate and butyrate along the reactor height at the steady states under four experimental conditions given in Table 1. The concentration gradients of substrates decreased with increasing recirculation flowrate or upflow velocity. But it should be noted that the analytical measurement of COD less than 100 mg/L might be less accurate.

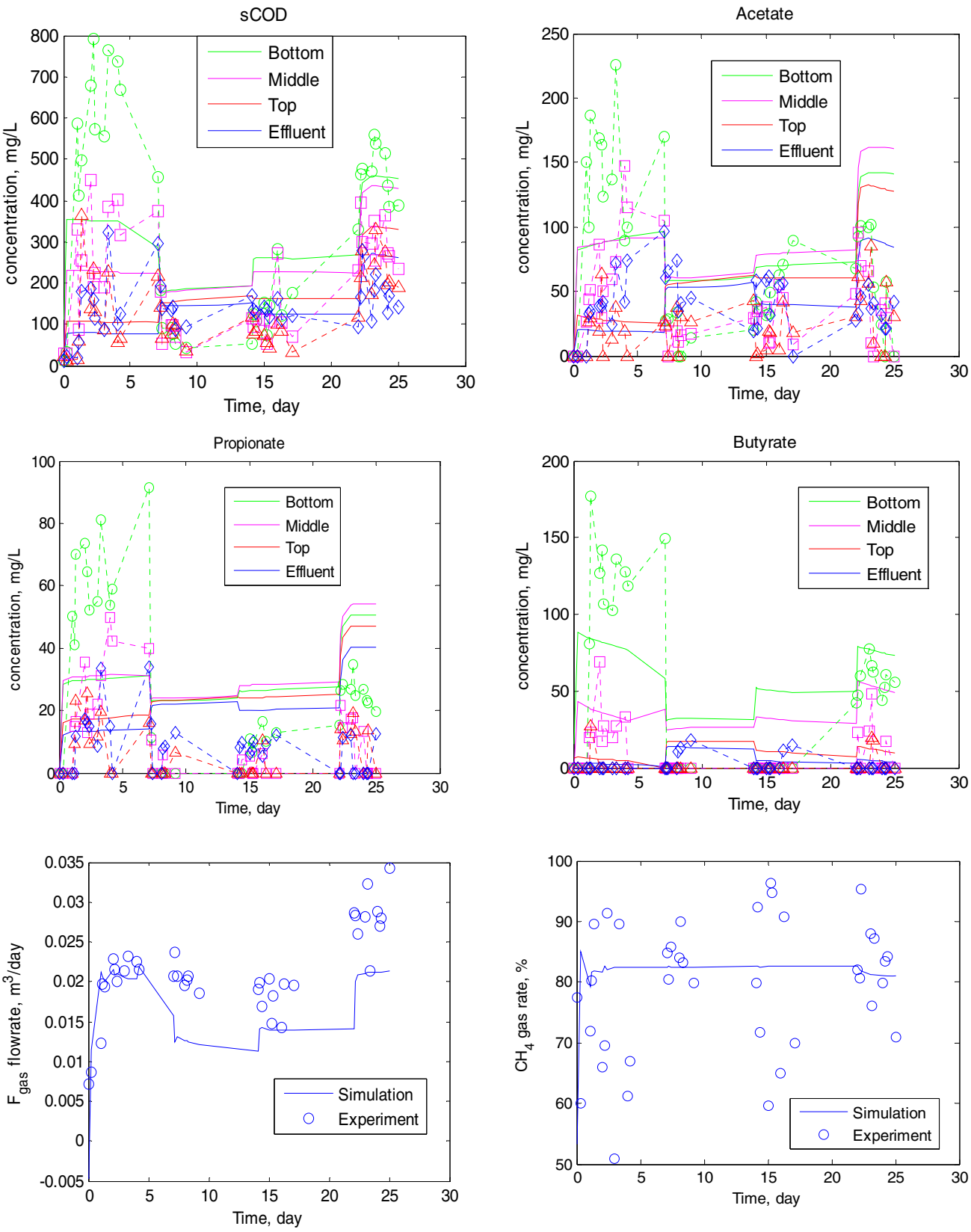

Figure 3 Comparison of the experimental data and the outputs of the distributed parameter model.

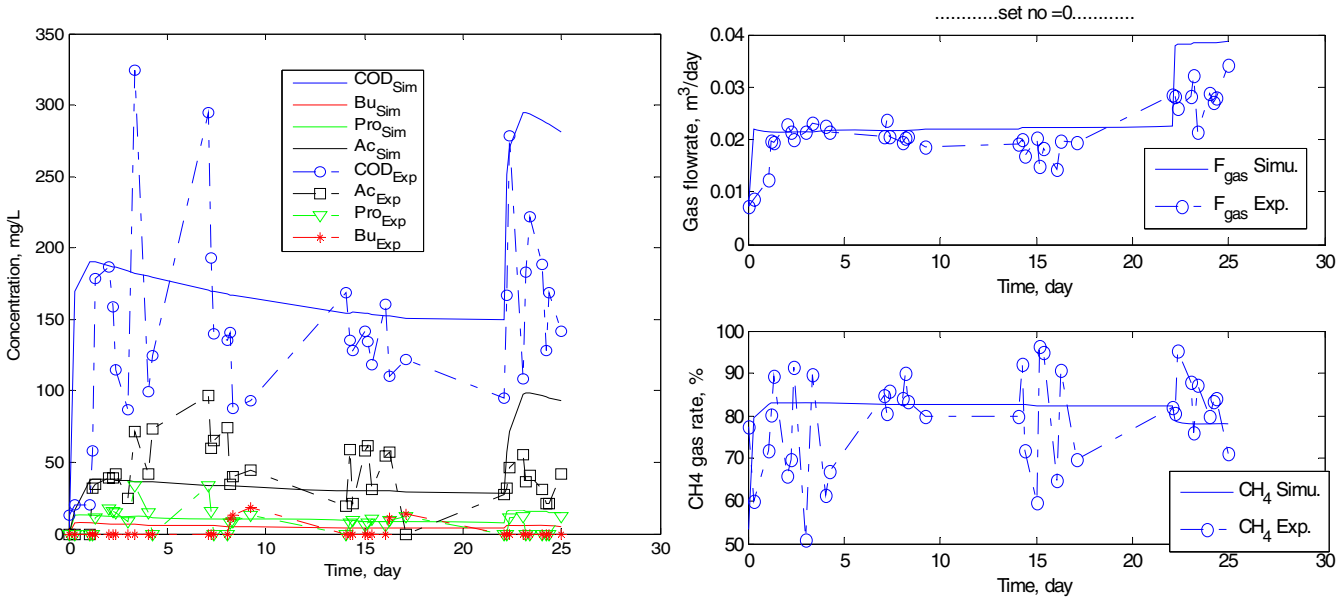

Figure 4 The comparison of experimental and CSTR (ADM1)-simulated sCOD, acetate, propionate, butyrate, gas rate and CH4%.

The distributed model calculated biomass distribution under all experimental conditions, as shown in Figure 5. Figure 5a shows total biomass with respect to the experimental time and Figure 5b shows profiles of the total biomass versus the reactor height. Obviously, low upflow velocity under the first experimental condition gave the largest biomass gradients along the axial position. The low upflow velocity also resulted in the lowest effluent biomass concentration under the same influent condition as other experiments. The experiments #1-3 had the same organic loading rate of 60 kg $m^{-3}day^{-1}$, the soluble COD removal efficiency increased as the upflow velocity decreased. The upflow velocity has a dominant effect on the component distribution and the effluent concentration. Both the substrate distribution in Figure 3 and the biomass distribution in Figure 5a reflected the same effects of the upflow velocity. High upflow velocity decreases the substrate gradients and increases the effluent substrate/biomass concentration, and vice versa. Figure 5b also illustrated that the concentration gradients of VSS would become small when the upflow velocity increased.

Apparently, recirculation increased the mixing in the liquid phase, and the contact between the soluble organic substrate and the biomass sludge, which increased the bio-reaction and COD biodegradation. In the treatment of high strength wastewater using a UASB reactor, it is beneficial to adopt an appropriate recirculation rate to dilute the influent wastewater. This helps to avoid the accumulation of substrates at the reactor bottom, such as volatile fatty acids, which could significantly drop the pH in the local area. Recirculation is an effective way to avoid the reaction inhibition due to high substrate concentration accumulated; it also lessens the pH inhibition and the usage of buffer (Olsson and Newell, 1999; Mshandete et al, 2004). Therefore, the distributed parameter model could describe the effect of recirculation flowrate on the reactor performance, which would be important in the design and operation of UASB-like reactors.

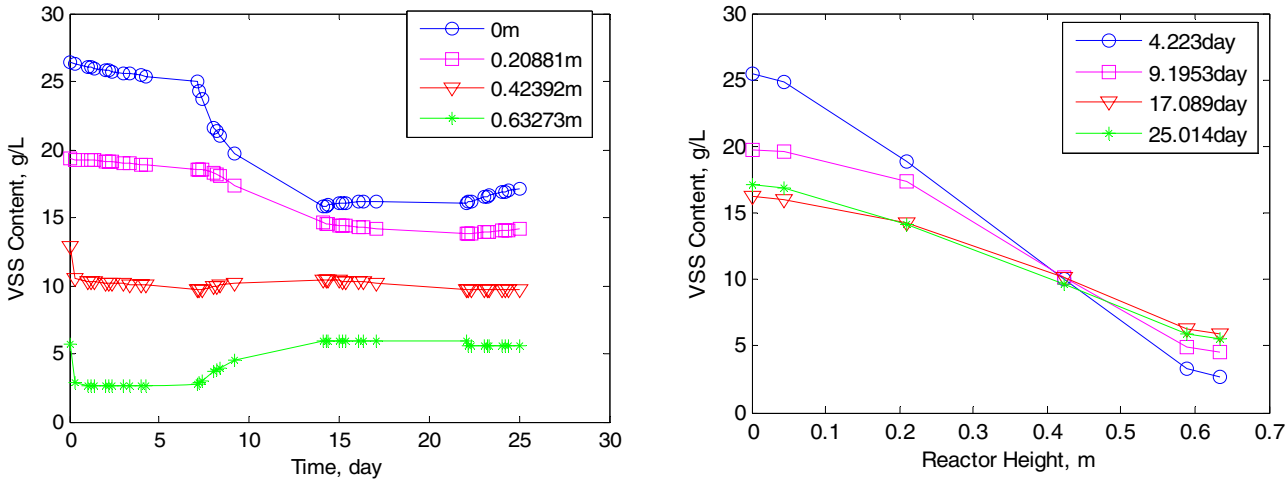

a b

Figure 5. Biomass profiles under the different operating conditions

CONCLUSION

In this work, a distributed parameter model is developed to simulate a UASB wastewater treatment process, based on the IWA ADM1. Based on process analysis, a total of twenty one model parameters were initially selected for parameter estimation. Sensitivity analysis allowed for selection of the five most sensitive parameters, which were identified using a numerical method. Using these estimated parameters, the distributed model simulated well the UASB process under different experimental conditions. The distributed model was able to show the distribution profiles of substrates along the reactor and simulate process response to the changes in upflow velocity. This cannot be achieved using the CSTR model.

The distributed parameter model can be used in developing new control strategies for UASB reactor, i.e. using upflow velocity to reduce the impact of organic overload on UASB reactor removal efficiency. Furthermore, the distributed model makes it possible to optimize the design and operation of UASB reactors by investigating the effect of biomass and substrate distribution on biodegradation performance.

ACKNOWLEDGEMENT

This work is funded by NRC-A*STAR Collaborative Research Program for BRI-NRC, Canada and Singapore-NRC Joint Research Programme (A*STAR Grant) for IHPC, Singapore.

REFERENCES

1. Kalyuzhnyi, S. V., V. I. Sklyar,M. A. Davlyatshina, S. N. Parshina, M. V. Simankova, N. A. Kostrikina & A. N. Nozhevnikova, Organic removal and microbiological features of uasb-reactor under various organic loading rates, Bioresource Technology 55 (1996) 47-54
2. Torkian, A., A. Eqbali, S.J. Hashemian, The effect of organic loading rate on the performance of UASB reactor treating slaughterhouse effluent, Resources, Conservation and Recycling (2003) 1 – 13
3. Sam-Soon, P., Loewenthal, R.E., Wentzel, M.C., Moosbrugger, R.E. and Marais G.R. Effects of a recycle in upflow anaerobic sludge bed (UASB) systems, Water SA., 17, 37-45 (1991)

4. Zeng, Y., S. J. Mu, S. J. Lou, B. Tartakovsky, S. R. Guiot, P. Wu, Hydraulic Modeling and Axial Dispersion Analysis of UASB Reactor, Biochemical Engineering Journal, (2005) 25, 113-123.
5. Batstone, D.J., J. Keller, R.I. Angelidaki, S.V. Kalyuzhnyi, S.G. Pavlostathis, A. Rozzi, W.T.M. Sanders, H. Siegrist and V.A. Vavilin, Anaerobic Digestion Model No.1, ISBN: 1900222787, IWA publishing, London, UK. 2002.
6. APHA AWWA and WEF, 1995. Standard methods for the examination of water and wastewater, American Public Health Association, Washington, DC.
7. Wayne J. Parker, Application of the ADM1 model to advanced anaerobic digestion, Bioresource Technology, 2005, in press.
8. Speece, R.E. (1996) Anaerobic biotechnology for industrial wastewaters, Archae press, Nashville, TN.
9. P. V. Danckwerts, Continuous flow systems -- Distribution of residence times. Chem. Eng. Sci. 2 (1953) 1-13.
10. Lee, T.T., F.Y. Wang, R.B. Newell, Dynamic modeling and simulation of activated sludge process using orthogonal collocation approach. Water Res. 33 (1999) 73-86.
11. Dochain, D. & Vanrolleghem, P.A., Dynamical Modelling and Estimation in Wastewater Treatment Processes. IWA publishing, 2001